24th INTERNATIONAL CONGRESS ON SOUND AND VIBRATION
23–27 July 2017, London

ICSV24
23-27JULY 2017
LONDON CALLING

IN-PLANE AND BENDING VIBRATION ANALYSIS OF A DOUBLE BOTTOM CABIN USING DYNAMIC STIFFNESS METHOD

Hui Li, W. W. Wu and X. W. Yin

National Key Laboratory on Ship Vibration & Noise, China Ship Scientific Research Center, 222 Shanshui East Road, Wuxi, China
email: lihui@cssrc.com.cn

In this study, the dynamic stiffness method, which yields exact solutions for plate structures, is employed to analyze the dynamics of ship structures. A dynamic stiffness formulation is developed for both in-plane and bending vibrations of plates with two opposite edges simply supported. Classical finite element technique is utilized to assemble local stiffness matrix into global coordinates to yield the dynamic stiffness matrix of a complete and complex structure. The method is then applied to an idealized model of a double bottom cabin structure as an example, within which both in-plane and bending vibration characteristics of the cabin can be clearly reproduced. Our numerical results are in good agreement with those calculated from finite element method, which demonstrates that this dynamic stiffness formulation has great potential in modelling the dynamics of built-up plate structures, especially in characterizing the in-plane waves, bending waves, and their mutual conversions along plate junctions.
Keywords: dynamic stiffness method; in-plane vibration; double bottom cabin structure

1. Introduction

Plates are extensively used as major components in various industrial structures, including ships, airplanes, building walls, and etc. In such engineering applications, plates are generally joined together along their junctions with specific angles, within which the longitudinal, shear and bending waves are transmitted. Particularly, these three waves can be converted into each other due to wave reflection and refraction[1], which makes the dynamic characteristics of the entire systems very complicated. Hence, there is an increasingly strong motivation for reliable prediction of the dynamic responses of plate structures.

Up to now, various DSM (dynamic stiffness method) elements have been developed for transverse or in-plane vibrations of plates. Wittrick and Williams proposed DSM in nineteen seventies based on classical plate theory[2]. Casimir et al. developed DSM elements for a plate with completely free boundary conditions[3], in which Gorman's superposition method[4,5]was employed to obtain the exact transverse displacements and the calculation of the forced vibrations for a single plate was demonstrated. Nefovska-Danilovic and Petronijevic[6]developed a dynamic stiffness matrix for isotropic rectangular plates with arbitrary conditions undergoing in-plane free vibrations.

However, compared to intensive research works on either bending or in-plane vibrations, the development of DSMs for them both was very limited. Bercin and Langley[1] extended Langley's work[7] to drive a dynamic stiffness matrix including in-plane vibrations for a plate with two opposite edges simply supported. Nevertheless, the dynamic stiffness matrix was not in an explicit form. Li et al.[8] derived the dynamic stiffness matrix considering both transverse and in-plane vibrations and investigated the forced vibrations of built-up plate structures. The recently developed DSMs for

thick and composite plates that account for shear deformation and rotatory inertia can generally include both in-plane and bending vibrations, but most of these works were only focused on the free vibrations or buckling.

The main objective of this work is to investigate both in-plane and bending vibration characteristics of a double-bottom cabin based on our newly developed dynamic stiffness formulation[8]. In Section 2, this dynamic stiffness method is briefly summarized, which mainly explains how both in-plane and bending vibrations of plates are incorporated into the dynamic stiffness matrix of plate element. Then in Section 3, our proposed method is applied to an idealized model of a double bottom cabin structure as an example. Our numerical results are in good agreement with those calculated from finite element method, which demonstrates that this dynamic stiffness formulation has great potential in modelling the dynamics of built-up plate structures, especially in characterizing the in-plane waves, bending waves, and their mutual conversions along plate junctions.

2. Brief review of dynamic stiffness method

2.1 Description of dynamic stiffness models for plate structures

For sake of completeness, our previous work is briefly summarized below. Shown in Fig.1 (a) is a conventional plate structure which consists of multiple plates. Adjacent plates are simply supported at their two opposite edges and rigidly joined along common edges.

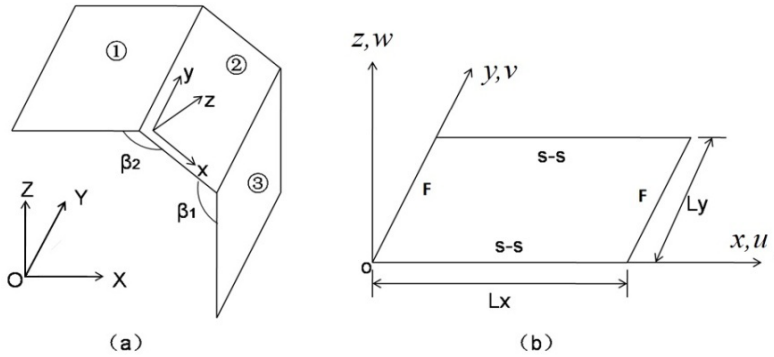

Fig. 1 (a) A built-up plate structure with arbitrarily oriented plates; (b) A rectangular plate with two opposite edges simply supported.

An individual plate shown in Fig. 1(b) is taken from the plate structure, to which the local coordinates oxyz are attached. The global coordinates OXYZ are independent of any specific local coordinates. Once the local dynamic stiffness matrix is derived, the overall dynamic stiffness matrix of the structure can be obtained by assembling all the local stiffness matrices after coordinate transformation.

2.2 Development of dynamic stiffness matrix in local coordinates

Without loss of generality, as illustrated in Fig.1 (b), the rectangular plate we select has the dimension of $L_x \times L_y$ and thickness h. It is simply supported along its two opposite edges while the other two edges are prescribed to be free. Based on the classical thin plate theory, the governing equations of the in-plane and bending motions of a plate are

$$\begin{cases} \dfrac{\partial^2 u}{\partial x^2} + a_1 \dfrac{\partial^2 u}{\partial y^2} + a_2 \dfrac{\partial^2 v}{\partial x \partial y} - \dfrac{\rho h}{B} \dfrac{\partial^2 u}{\partial t^2} = 0 \\ \dfrac{\partial^2 v}{\partial y^2} + a_1 \dfrac{\partial^2 v}{\partial x^2} + a_2 \dfrac{\partial^2 u}{\partial x \partial y} - \dfrac{\rho h}{B} \dfrac{\partial^2 v}{\partial t^2} = 0 \\ \nabla^4 w + \dfrac{\rho h}{D} \dfrac{\partial^2 w}{\partial t^2} = 0 \end{cases} \tag{1}$$

where u, v and w are the displacements in x-, y- and z-directions. The parameters in Eq. (1) are defined as

$$a_1 = \frac{1-\mu}{2}, a_2 = \frac{1+\mu}{2}, B = \frac{Eh}{1-\mu^2}, D = \frac{Eh^3}{12(1-\mu^2)} \tag{2}$$

where B and D are the extension rigidity and flexural rigidity, respectively. E, ρ, and μ are Young's modulus, density and Poisson's ratio. The damping of material is taken into account by introducing complex modulus of elasticity, namely, $E_C = E(1+i\cdot\delta),$ where $\delta = 2\eta$ is damping loss factor, η is damping ratio.

For simply supported boundary conditions along their two opposite edges, namely, $\mathrm{y} = 0$ and $\mathrm{y} = L_{\mathrm{y}}$, we have $u = 0$ and $w = 0$, but $v \neq 0$. Therefore, the in-plane and out-of-plane displacements, respectively, can be expressed in terms of Levy series,

$$\begin{cases} u(x,y,t) = \sum_{n=1}^{N} U_n(x)\sin(k_n y)e^{i\omega t} \\ v(x,y,t) = \sum_{n=1}^{N} V_n(x)\cos(k_n y)e^{i\omega t} \\ w(x,y,t) = \sum_{n=1}^{N} W_n(x)\sin(k_n y)e^{i\omega t} \end{cases} \tag{3}$$

where N is the truncation number, k_n is wavenumber in y direction that can be written as $k_n = n\pi / L_y$. For sake of brevity, the time dependence $e^{i\omega t}$ will be suppressed hereafter. In reference[8], Leissa's solutions for bending vibrations[9], together with Becin and Langley's[1] accurate expressions for in-plane vibrations are employed, as a result, the internal forces within the plate, including extensional forces, in-plane and transverse shear forces, and bending moments, can be readily derived.

In order to obtain the dynamic stiffness matrix, the displacements and forces at the junctions, i.e, x=0 and x=Lx, shall be derived beforehand, which can be arranged in the following forms, respectively,

$$q = \{u_1, v_1, w_1, \theta_1, u_2, v_2, w_2, \theta_2\}^T \tag{4a}$$

$$Q = \{N_{xx1}, N_{xy1}, Q_{x1}, M_{xx1}, N_{xx2}, N_{xy2}, Q_{x2}, M_{xx2}\}^T \tag{4b}$$

where the subscript 1 denotes x=0 while 2 corresponds to x=Lx, and $\theta = -\frac{\partial w}{\partial x}$. With reference to the convention of displacements and forces, Eq. (4) can be rewritten in more details,

$$\begin{aligned} q &= [u(0,y) \quad v(0,y) \quad w(0,y) \quad \theta(0,y) \quad u(L_x,y) \quad v(L_x,y) \quad w(L_x,y) \quad \theta(L_x,y)]^T \\ Q &= [N_{xx}(0,y) \quad N_{xy}(0,y) \quad Q_x(0,y) \quad M_{xx}(0,y) \quad -N_{xx}(L_x,y) \quad -N_{xy}(L_x,y) \quad -Q_x(L_x,y) \quad -M_{xx}(L_x,y)]^T \end{aligned} \tag{5}$$

In the present paper, using Projection method, expressions for the displacements and forces in Eq. (5) can be transformed into generalized displacements $\overline{q} = [\overline{q}_1, \cdots, \overline{q}_n, \cdots, \overline{q}_N]_{8\times N}$ and generalized forces $\overline{F} = [\overline{F}_1, \cdots, \overline{F}_n, \cdots, \overline{F}_N]_{8\times N}$, respectively. By combining the expressions for generalized displacements and forces, the following relationship between them can be readily obtained, leading to the dynamic stiffness matrix $\overline{K}_D$ of a plate element.

$$\overline{F} = \overline{K}_D(\omega)\overline{q} \tag{6}$$

2.3 Coordinate transformation and assembly procedure of global dynamic stiffness matrix

The dynamic stiffness matrix derived in the previous subsection is expressed in local coordinates, which can be termed as local dynamic stiffness matrix. In order to obtain the dynamics of the entire plate structures, first, local dynamic stiffness matrix for each plate shall be transformed into global coordinates.

The global and local coordinates systems for the plate structures are illustrated in Fig.1. By assuming that the local coordinate system oxyz can be obtained by rotating OXYZ system about Y axis by an angle θ, then the transformation of the displacements and forces at any nodes from global coordinates to local is obtained by a matrix T which can be expressed as,

$$T = \begin{bmatrix} \Lambda & 0 \\ 0 & \Lambda \end{bmatrix} \tag{7}$$

$$\Lambda = \begin{bmatrix} \cos\theta & 0 & -\sin\theta & 0 \\ 0 & 1 & 0 & 0 \\ \sin\theta & 0 & \cos\theta & 0 \\ 0 & 0 & 0 & 1 \end{bmatrix} \tag{8}$$

Therefore, for a plate substructure, the relationship between the generalized displacements in global coordinates $\overline{q}^g$ and in local coordinates $\overline{q}$ is written as,

$$\overline{q} = T\overline{q}^g \tag{9}$$

Similarly, the transformation of generalized forces is,

$$\overline{F} = T\overline{F}^g \tag{10}$$

Accordingly, the transformation of stiffness matrix is expressed as follows,

$$\overline{K}_D{}^g = T^T\overline{K}_D T \tag{11}$$

where $\overline{K}_D$ and $\overline{K}_D{}^g$ are the dynamic stiffness matrix for a plate substructure in local and global coordinates, respectively. Next, the transformed stiffness matrix $\overline{K}_D{}^g$ shall be assembled into overall dynamic stiffness matrix by using standard finite element techniques. The assembly procedure is the same as that in FEM, except that the degrees of freedom for plates correspond to lines instead of nodes.

3. Numerical results and discussion

In this section the above mentioned theory is applied on an idealized model of a double bottom cabin structure. The structure, consisting of nineteen plates is shown in Fig. 2. The widths of the nineteen plates, respectively, (in meters) are: 1.75, 2.5, 1.75, 2.2, 6, 2.2, 0.8, 0.414, 0.414, 0.414, 0.95, 1.6, 2.5, 1.6, 0.95, 0.414, 0.414, 0.414, 0.8, and the length is 10. The thickness of the plates (in millimeters) are 10, 10, 10, 8, 8, 8, 14, 14, 14, 14, 14, 12, 14, 12, 14, 14, 14, 14, 14. Each plate is simply supported at its two longitudinal edges, and the other two transverse edges, which are the coupled edges, are prescribe to be free. Each member of the structure is taken to be steel, which has the material parameters listed in Table 1.

Table 1: Material parameters of the double bottom cabin

E(Gpa)	ρ (Kg/m^3)	μ	η
200	7850	0.33	0.002

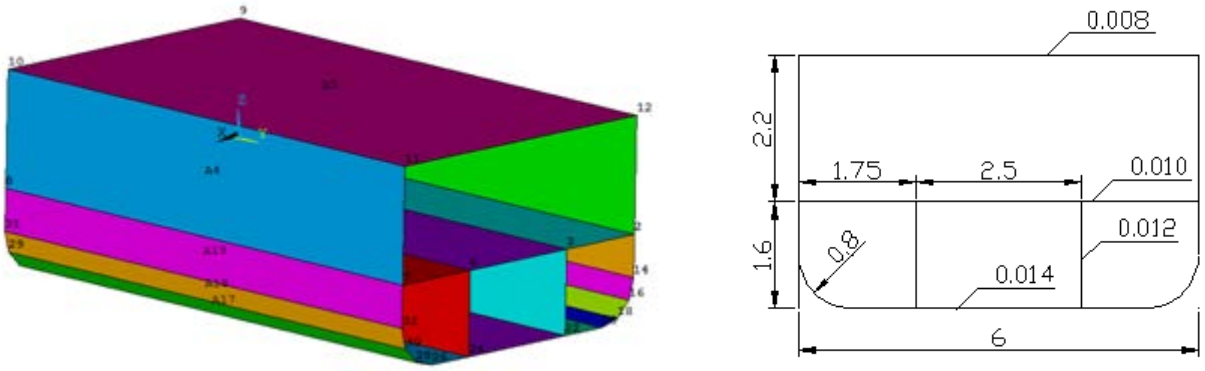

(a) (b)

Fig. 2 (a) FEM model of the double bottom cabin structure; (b) Front view of the double bottom cabin structure

In this paper, validation works are updated so as to further confirm that our proposed DSM can present accurate results for both in-plane and out-of-plane vibrations of complex cabin structures, even in very high frequencies. The computation frequency range covers from 0 Hz to 5,000 Hz. With reference to the suggestions from Li et al [8], the truncation number N for DSM is set to be 10, and finite sizes for the plates are prescribed to be $0.2m \times 0.2m$ and $0.1m \times 0.1m$, respectively. As shown in Fig. 3, two types of harmonic loadings are applied onto one of the inner bottom plates so that the in-plane and bending vibrations can be excited, including uniformly distributed transverse forces and an unit concentrated force. The concentrated force is loaded in 2/5 of the length edge, and the observation point A is located in 1/5 of the length edge.

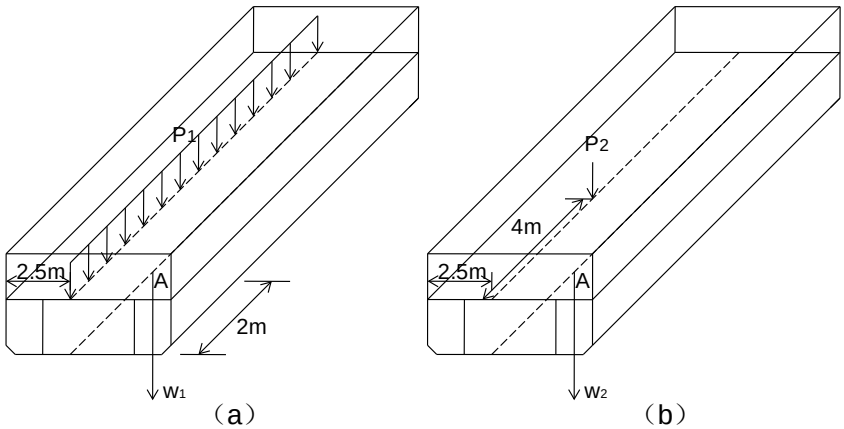

Fig. 3 Schematic illustration of forces applied to the double bottom cabin structure

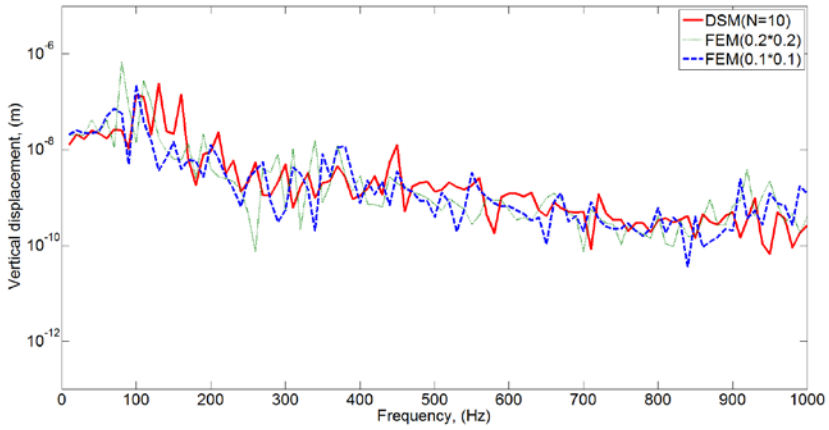

(a)

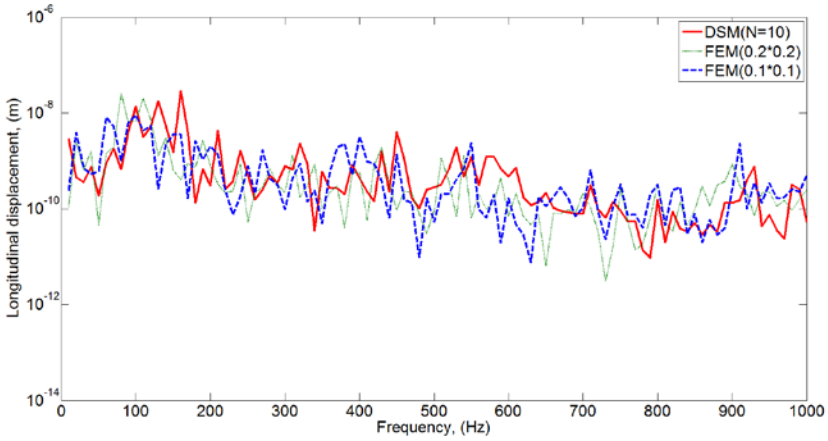

(b)

Fig. 4 (a) Transverse responses at point A due to distributed transverse forces; (b) In-plane responses at point A due to distributed transverse forces.

When transverse forces with amplitude of 1 N/m are enforced onto the plates, vertical (or transverse) displacements and longitudinal displacements are examined so as to evaluate whether our DSM can accurately reproduce bending and in-plane vibrations. Shown in Fig. 4 (a) are the results for the transverse displacement responses at point A over the frequency range of [0-1,000Hz], which are obtained by using our method and FEM, respectively. As we can see, there are discrepancies in the resonance frequencies between them. When computation frequency is increasing, uncertainties arise in FEM analysis, as a result, considerable variation in responses will appear due to slight variations in geometry, materials, boundary conditions, or even meshing schemes. Hence, despite discrepancies in resonance frequencies, it's acceptable to find that the responses from FEM and from DSM have the same trend, and lie in the same level.

Similarly, shown in Fig. 4 (b) is the comparison of the curves for the in-plane dynamic responses at point A obtained by using DSM and FEM. We can also find that our DSM results for the in-plane responses agree well with all FEM results except those obtained from the FEM model with $0.2m \times 0.2m$ elements. Hence, from Fig. 4 (a) and Fig. 4 (b), we can deduce that our method can successfully present good results for both transverse and in-plane vibrations. Moreover, it is demonstrated that the conversion from transverse vibrations to in-plane vibrations is correctly implemented by using our DSM approach.

In order to examine the capability of our method in dealing with higher frequencies, the frequency range for vibration analysis is extended to [0-5,000 Hz]. When the computation frequency range is increasing, it's reasonable to use larger truncation number N so that higher vibration modes can be superposed into overall dynamic responses. It is indicated that the results agree quite well over a very broad frequency range as much as 5,000 Hz. This capability is very appealing to scientists who are struggling with the structural dynamics in medium or even high frequencies.

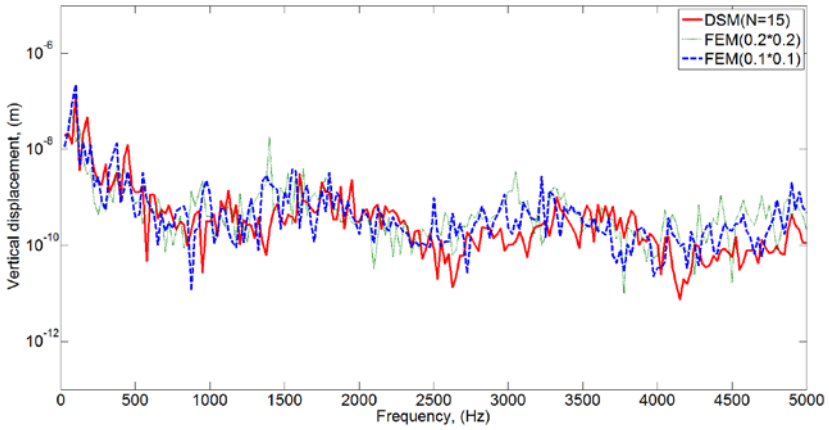

(a)

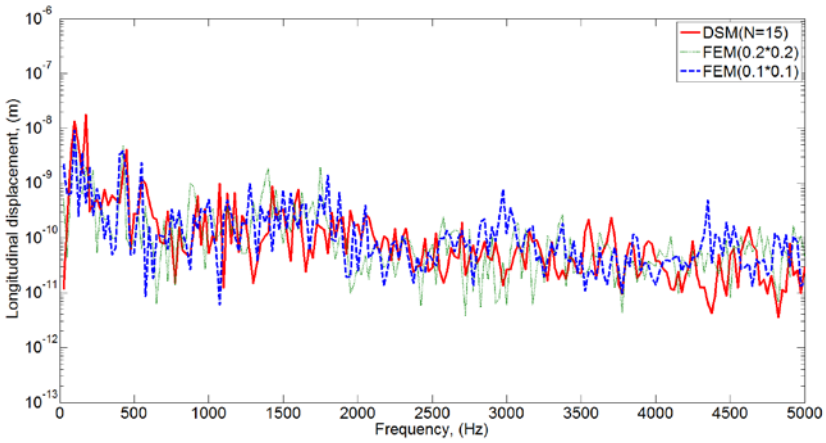

(b)

Fig.5 (a) Transverse responses at point A due to distributed transverse forces within 5,000Hz; (b) In-plane responses at point A due to distributed transverse forces within 5,000Hz.

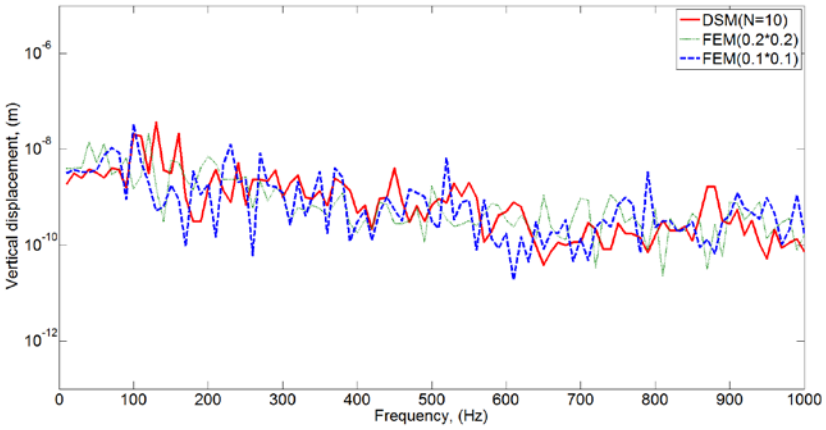

(a)

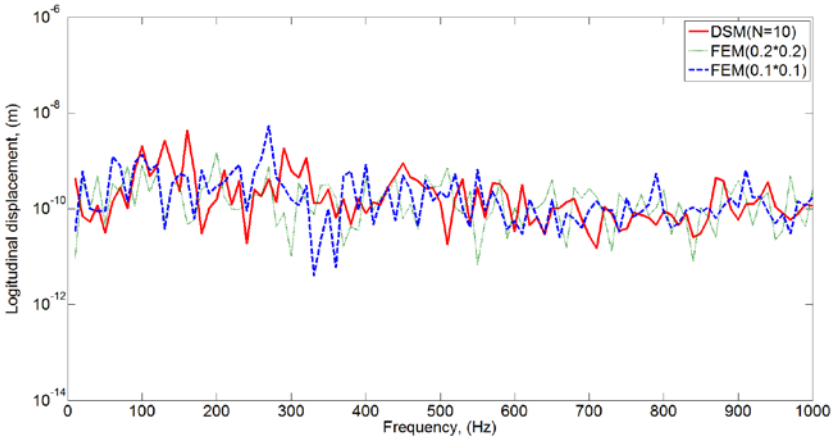

(b)

Fig.6 (a) Transverse responses at point A due to a unit concentrated force; (b) In-plane responses at point A due to a unit concentrated force.

The second load case, which is illustrated in Fig. 3 (b), is designated to apply an unit concentrated force P_2 with amplitude of 1N. It is shown in Fig. 6 that our results for the transverse and longitudinal displacements at point A agree well with those obtained by FEM below 1,000 Hz. We admit that there are some discrepancies in the resonance frequencies and vibration amplitude. However, our DSM results for the vibration displacements have the same trend with FEM results.

In this subsection, through the above two cases, the capabilities of our DSM are validated. We can conclude that both bending vibrations and longitudinal vibrations can be accurately modelled by this method. The number of plate elements in the present solution is 19, while the number of

elements in the finite element models is respectively 7,020 and 28,084. Consequently, using the dynamic stiffness model significantly decreases memory requirement and computational time, and yet retaining high accuracy and high efficiency of the results. The comparison of computation between DSM and FEM is listed in Table 2. But we have to remind that convergence analysis with respect to different truncation numbers shall be made prior to using our DSM, especially in high frequency range.

Table 2: Comparison of computation between DSM and FEM

	Number of element	Frequency range	Computational time
DSM	19	No frequency limit	10min within 10kHz
FEM	7020/28084	Limited by high frequency	1.5h within 10kHz

4. Conclusions

By accounting for both in-plane and bending vibrations, the dynamic stiffness formulation for the plate structures, which are simply supported at their opposite edges, is used for vibration analysis of a cabin structure which represents a portion of a ship foundation. Accurate results and considerably higher efficiency are obtained, which demonstrates that our proposed DSM approach has great potentials in modeling the dynamics of complex built-up plate structures. This makes it possible to correctly address the wave conversions between in-plane and out-of-plane motions within plates.

This work was financially supported by China Ship Scientific Research Center Fund (Reference No.: J1668).

REFERENCES

1 Bercin AN, Langley RS (1996), Application of the dynamic stiffness technique to the in-plane vibrations of plate structures. *Computers and Structures,* 59 (5) :869-875.

2 W.H. Wittrick, F.W. Williams, Buckling and vibration of anisotropic or isotropic plate assemblies under combined loadings, *International Journal of Mechanical Sciences* 16 (4) (1974) 209–239.

3 J.B. Casimir, K. Kevorkian, and T. Vinh, The dynamic stiffness matrix of two-dimensional elements: application to Kirchhoff's plate continuous elements, *Journal of Sound and Vibration,* 287 (2005) 571–589.

4 D.J. Gorman, Free Vibration Analysis of Rectangular Plates, Elsevier, Amsterdam, 1982.

5 D.J. Gorman. Free vibration analysis of the completely free rectangular plate by the method of superposition, *Journal of Sound and Vibration,* 57(3)(1978) 437–447.

6 M. Nefovska-Danilovic and M. Petronijevic, In-plane free vibration and response analysis of isotropic rectangular plates using the dynamic stiffness method, *Computers and Structures*, 152 (2015) 82-95.

7 R.S. Langley, Application of the dynamic stiffness method to the free and force vibrations of aircraft panels, *Journal of Sound and Vibration,* 135 (1989) 319-331.

8 Hui Li, X.W. Yin, W.W. Wu, Dynamic stiffness formulation for in-plane and bending vibrations of plates with two opposite edges simply supported. *Journal of Vibration and Control,* 2016.

9 Leissa A (1993), Vibration of plates. Woodbury, New York: Acoustical Society of America.